Gaze Orienting in Dynamic Visual Double Steps

Joyce Vliegen, Tom J. Van Grootel and A. John Van Opstal

JN 94:4300-4313, 2005. First published Aug 17, 2005; doi:10.1152/jn.00027.2005

J Neurophysiol 94: 4300–4313, 2005.
First published August 17, 2005; doi:10.1152/jn.00027.2005.

Gaze Orienting in Dynamic Visual Double Steps

Joyce Vliegen, Tom J. Van Grootel, and A. John Van Opstal
Department of Medical Physics and Biophysics, Radboud University Nijmegen, Nijmegen, The Netherlands

Submitted 10 January 2005; accepted in final form 11 August 2005

Vliegen, Joyce, Tom J. Van Grootel, and A. John Van Opstal. Gaze orienting in dynamic visual double steps. *J Neurophysiol* 94: 4300–4313, 2005. First published August 17, 2005; doi:10.1152/jn.00027.2005. Visual stimuli are initially represented in a retinotopic reference frame. To maintain spatial accuracy of gaze (i.e., eye in space) despite intervening eye and head movements, the visual input could be combined with dynamic feedback about ongoing gaze shifts. Alternatively, target coordinates could be updated in advance by using the *preprogrammed* gaze-motor command ("predictive remapping"). So far, previous experiments have not dissociated these possibilities. Here we study whether the visuomotor system accounts for saccadic eye–head movements that occur during target presentation. In this case, the system has to deal with fast dynamic changes of the retinal input and with highly variable changes in relative eye and head movements that cannot be preprogrammed by the gaze control system. We performed visual–visual double-step experiments in which a brief (50-ms) stimulus was presented during a saccadic eye–head gaze shift toward a previously flashed visual target. Our results show that gaze shifts remain accurate under these dynamic conditions, even for stimuli presented near saccade onset, and that eyes and head are driven in oculocentric and craniocentric coordinates, respectively. These results cannot be explained by a predictive remapping scheme. We propose that the visuomotor system adequately processes dynamic changes in visual input that result from self-initiated gaze shifts, to construct a stable representation of visual targets in an absolute, supraretinal (e.g., world) reference frame. Predictive remapping may subserve transsaccadic integration, thus enabling perception of a stable visual scene despite eye movements, whereas dynamic feedback ensures accurate actions (e.g., eye–head orienting) to a selected goal.

INTRODUCTION

This paper concerns the transformations underlying the programming of two-dimensional (2D) head-free gaze shifts to visual targets. Gaze is the orientation of the visual axis in space, defined by the sum of the orientations of the eye in the head and the head in space.

In studies of the gaze control system the typical situation is one in which eye and head orientations are initially aligned (exceptions are, e.g., Goossens and Van Opstal 1997b; Stahl 2001; Volle and Guitton 1993). Under such conditions, there is a one-to-one correspondence between the retinal location of a briefly flashed visual stimulus and the motor commands for eyes and head to acquire the target. However, under more natural conditions, the eyes are not fixed in the head. Eyes and head may then not point in the same direction, and make different intervening movements before the orienting response. As illustrated in Fig. 1, in such cases the initial retinal error ($T_{E,0}$) no longer suffices as a valid motor command for eyes and head (e.g., Goossens and Van Opstal 1997b). Instead, the correct motor errors ($T_{E,2}$ and $T_{H,2}$, respectively) require different transformations of the target location that incorporate both the eye–head misalignment and the intervening eye–head movements.

The gaze control system could implement these transformations in a variety of ways. For example, it could use preprogrammed (feedforward) information about the upcoming gaze shift. Alternatively, it could rely on continuous dynamic feedback about the actual movements of eyes and head.

To study these different transformations we have elicited eye–head saccades to visual stimuli that were briefly flashed *during* an intervening eye–head gaze shift.

Static double steps

Our paradigm contrasts with the classic saccade double-step experiment, which we here denote as the *static* double step (Fig. 2*A*). In that experiment two peripheral targets are presented shortly after each other, but *before* the initiation of the first gaze shift. The subject is instructed to foveate both targets at the remembered spatial locations in the order of their appearance. The double-step paradigm has been used in a number of (head-fixed) saccadic eye-movement studies (Becker and Jürgens 1979; Goossens and Van Opstal 1997a; Ottes et al. 1984), all of which showed that saccades toward the second target fully account for the size and direction of the first eye movement. Several theories to explain this result have been forwarded in the literature.

Position versus displacement feedback

Neurophysiological studies have demonstrated that the primate visuomotor system also compensates for an intervening saccade evoked by microstimulation of the midbrain superior colliculus (SC; Mays and Sparks 1980; Sparks and Mays 1983). These studies suggested that the retinal location of the target is transformed into a head-centered reference frame, in which the system can readily program the future saccade by incorporating eye-in-head position (Sparks and Mays 1983; Van Gisbergen et al. 1981; Zipser and Andersen 1988). However, lack of evidence for a head-centered representation of visual targets, together with the idea that the SC represents saccades in an eye-centered, rather than in a head-centered motor map (Robinson 1972; Sparks and Mays 1983), has prompted others to propose an eye-displacement updating scheme to explain these results. In this scheme, the visuomotor system keeps targets in an eye-centered reference frame, while updating the saccade plan with feedback about intervening eye

Address for reprint requests and other correspondence: A. J. Van Opstal, Department of Medical Physics and Biophysics, Radboud University Nijmegen, Geert Grooteplein 21, 6525 EZ Nijmegen, The Netherlands (E-mail: j.vanopstal@science.ru.nl).

The costs of publication of this article were defrayed in part by the payment of page charges. The article must therefore be hereby marked "*advertisement*" in accordance with 18 U.S.C. Section 1734 solely to indicate this fact.

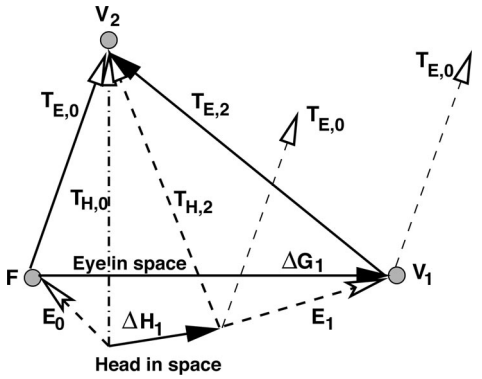

FIG. 1. In head-free gaze shifts, eye and head are typically unaligned, and make movements of different amplitudes, thus creating different error signals for a visual target. Scheme shows a fixation point (F), a first visual stimulus (V_1), and a second visual target (V_2), both presented before the eye (ΔG_1) –head (ΔH_1) movement toward V_1. At the start of the trial, the eye-in-head position is E_0. Initial retinal error for V_2 is $T_{E,0}$, but for the head it is different: $T_{H,0}$. After the first gaze shift, the eye-in-head position has changed (E_1) and the motor errors for eye ($T_{E,2}$) and head ($T_{H,2}$) are very different from the original retinal error, $T_{E,0}$. They depend on the intervening eye–head gaze shift for the eye-in-space ($T_{E,2} = T_{E,0} - \Delta G_1$) and on the eye–head misalignment and head (or eye–head) movement for the head-in-space ($T_{H,2} = T_{E,0} + E_0 - \Delta H_1 = T_{E,0} + E_1 - \Delta G_1$), respectively.

displacement (Jürgens et al. 1981). Neurophysiological recordings in the primate frontal eye fields (FEFs) provided support for this alternative model by demonstrating that FEF cells carry the signals required for this transformation (Goldberg and Bruce 1990). Note that both schemes incorporate dynamic feedback of actual motor performance to update the future response.

Feedforward versus feedback

More recent studies, however, have suggested that at different stages within the visuomotor pathway a coordinate transformation may already be performed *before* the initiation of the first saccade [so-called predictive remapping; posterior parietal cortex (PPC): Colby et al. 1995; Duhamel et al. 1992; FEF: Umeno and Goldberg 1997; SC: Walker et al. 1995]. Such a feedforward mechanism could provide a neural correlate for trans-saccadic integration, which is thought to underlie the percept of a stable visual environment, despite saccadic eye movements that sweep the visual scene across the retina (Duhamel et al. 1992). However, such a mechanism could also underlie spatially accurate performance of saccades in the double-step paradigm.

In Fig. 2, we have outlined two slightly different versions of the predictive remapping idea: in the *visual-predictive* (VP) model the initial retinal target representation ($T_{E,0}$) is updated on the basis of the retinal coordinates of the first visual target (FV_1), whereas the *motor-predictive* (MP) model relies on an efference copy of the planned first gaze shift (ΔG_1). Because the VP scheme is based on visual information only, it does not account for a possible localization error of the first target, in contrast to the MP model. This results in slightly different predictions for the response to the second target. So far, neurophysiological recordings do not allow a distinction between these two alternatives.

According to the feedback model (FB), the retinal error of the second target (T_E) is continuously updated with information about eye and head movements through *dynamic feedback* from the gaze control system. In this way, the motor errors that will drive the eye and head are always accurate.

The static double-step paradigm (Fig. 2*A*), in which both targets are presented before the eye–head movement onset, cannot dissociate updating schemes based on dynamic feedback from those based on predictive remapping. Although the VP model predicts a localization error that depends on the error for the first target, both the MP and the FB models predict equally accurate localization responses.

Dynamic double steps

In the present study we have applied a dynamic double-step paradigm, in which the second target is presented in midflight of the first, intervening gaze shift (ΔG_1, Fig. 2*B*). If predictive remapping would underlie the programming of the future gaze shift, systematic errors are expected in this paradigm (VP, MP vectors) because, in these models, the system is supposed to update the initial retinal input on the basis of prior (i.e., preprogrammed) information about the entire first gaze shift. According to the MP model, the target is missed by the difference between the full gaze shift and the partial movement after the onset of the second target, ΔG^*. For the VP model, this localization error corresponds to the difference between vector FV_1 and ΔG^*. The feedback model (FB), however, predicts accurate performance under all stimulus conditions.

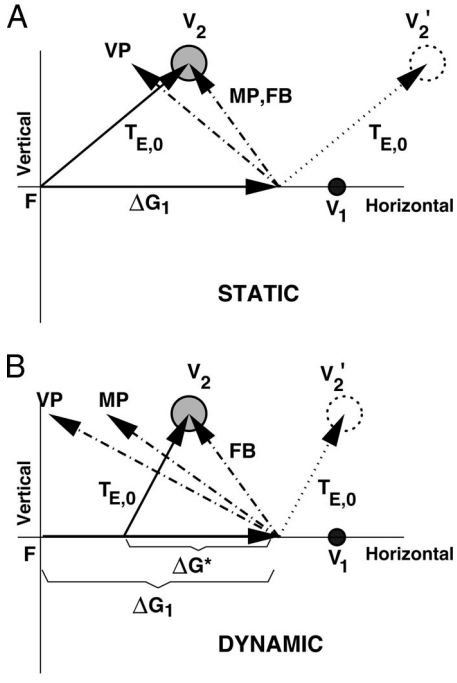

FIG. 2. Schematic outline of the 2 different double-step experiments in this study, showing a fixation point (F), 2 visual targets (V_1 and V_2), the first gaze shift (ΔG_1, which is here assumed to undershoot the first target), and the predicted second gaze shift according to 3 models. Head movement is not shown, for clarity. $T_{E,0}$ is the initial retinal error of V_2. V_2' is the retinal position of V_2 after ΔG_1. *A*: static double step. Targets are presented before the first gaze shift onset. Vector VP represents the response of the visual predictive model (update based on vector FV_1). Motor predictive (MP) model and the dynamic feedback (FB) model both predict accurate localization (update based on actual ΔG_1). *B*: dynamic double step. V_2 is presented during the first gaze shift, which dissociates the MP and FB models. MP model still uses the full first gaze shift to update the target, whereas the FB model incorporates only the partial gaze shift after the onset of the second target.

Related studies

Interestingly, Hallet and Lightstone (1976) applied a dynamic paradigm for horizontal eye movements, and reported accurate secondary saccades. However, later studies showed that both visual perception and oculomotor programming can be strongly influenced by concomitant saccades. For example, systematic inaccuracies in stimulus localization arise when dim targets are briefly flashed in darkness around the onset of a saccade (Dassonville et al. 1995; Schlag and Schlag-Rey 2002). These errors, which could be as large as 70% of the saccade amplitude, were attributed to the use of a low-pass–filtered representation of eye position in updating target locations (Dassonville et al. 1992; Schlag et al. 1989). According to this idea, the response endpoints in Fig. 2*B* would systematically shift from V_2' (no compensation) to V_2 (full compensation) as a function of the stimulus timing relative to first-saccade onset.

Moreover, under photopic stimulus conditions saccades cause a considerable perceptual deformation of the visual field that leads to systematic misjudgments about stimulus locations (Bremmer and Krekelberg 2003; Lappe et al. 2000; Ross et al. 1997).

These latter studies suggest that the observed mislocalizations could be attributable to visual-perceptual factors, rather than to a property of sensorimotor integration. Note that that an inaccurate representation of oculomotor feedback signals would also induce mislocalizations of nonvisual stimuli, such as sounds. We recently studied eye–head gaze shifts to brief sounds presented under static and dynamic visual–auditory double steps, and showed that sound localization behavior remained accurate for all conditions (Vliegen et al. 2004). That study therefore suggested that the motor feedback signals are accurate.

The present paper extends these previous studies in a number of ways. First, with the notable exception of a few studies (Goossens and Van Opstal 1997b; Ron et al. 1993, 1994; Volle and Guitton 1993), eye–head coordination performance in double steps has hardly been studied so far. Moreover, these studies were all confined to static double steps. As may be appreciated from the schematic outline in Fig. 1, head-free gaze shifts in dynamic double steps poses far from trivial problems to the gaze-control system. Because the eyes and head move toward the initial visual target at highly variable and different velocities, at different relative latencies, and with different amplitudes, the eye and head motor errors at the time of stimulus presentation are essentially unpredictable. This property provides a serious challenge for gaze-control strategies based on predictive remapping.

Second, our experiments also relate to the ongoing dispute, described above, about absolute position coding of visual targets in an supraretinal reference frame (e.g., head-centered; Mays and Sparks 1980; Sparks and Mays 1983; Van Gisbergen et al. 1981; Zipser and Andersen 1988; or even body-centered; Andersen 1997; Kopinska and Harris 2003; Xing and Andersen 2001), versus relative displacement coding of target locations in an eye-centered reference frame (Colby et al. 1995; Duhamel et al. 1992; Goldberg and Bruce 1990; Jürgens et al. 1981; Nichols and Sparks 1995). Third, visual and auditory targets are initially encoded in different reference frames. Because auditory targets are encoded in a head-centered reference frame, the sound-localization cues become dynamic as a result of *head* movements. In contrast, visual targets are encoded in a retinotopic reference frame, inducing fast dynamic changes of the retinal input as a result of *eye* movements. Thus for accurate movements of eyes and head to audiovisual stimuli, the modality-specific reference frames need to be updated dynamically on extremely short timescales, but with different transformation rules for eyes and head (Goossens and Van Opstal 1997b).

Our experiments show that 2D eye–head coordination is equally accurate under static and dynamic visual double steps, although we noted subtle differences with our recent auditory localization study. Further, we obtained no large systematic localization errors when the visual stimulus fell around the onset of the first saccadic gaze shift. We propose a target-updating scheme in which the programming stage of the gaze control system operates under continuous feedback, using accurate information about instantaneous eye and head movements. We discuss our findings in terms of current models of gaze control and target updating, and argue that our data are hard to reconcile with a pure displacement feedback scheme in which visual targets remain in an eye-centered reference frame.

METHODS

Subjects

Nine subjects (four females, five males; ages 20–46) participated in the experiments. All had normal vision except for JO, who is amblyopic in his right, recorded eye. All subjects had oculomotor and head-motor responses within the normal range. Subjects MK, ML, MV, MW, RK, and SP were kept naive about the exact goal of this study. The authors (JO, JV, TG) participated in all parts of the experiments. Subject RK participated only in the first target configuration (see following text) and subjects MK, ML, MV, MW, and SP only in the second target configuration. Informed consent was obtained from all participants. Experiments adhered to the principles of the Declaration of Helsinki, and the U.S. federal regulations for the Protection of Human Subjects.

Apparatus and stimuli

Experiments were conducted in a completely dark (<0.001 cd/m^2, measured with a Minolta LS-100 luminance meter), sound-attenuated room ($3 \times 3 \times 3$ m^3). The subject was seated comfortably on a chair in the center of the room with firm support in the back and lower neck. Viewing was binocular. The subject faced a thin-wire hemisphere with a radius of 0.85 m, the center of which coincided with the center of the subject's head. On this hemisphere 85 red/green light-emitting diodes (LEDs; Knightbright Electronics, L59EGW/CA) were mounted at seven visual eccentricities $R = [0, 2, 5, 9, 14, 20, 27, 35]$ deg relative to the straight-ahead viewing direction (defined in polar coordinates as $[R, \phi] = [0, 0]$ deg), and at 12 different directions, given by $\phi = [0, 30, \ldots, 330]$ deg, where $\phi = 0$ deg is rightward from the center and $\phi = 90$ deg is upward. The hemisphere was covered with thin black silk.

Stimuli were delivered by the red LEDs ($\lambda = 625$ nm) that had a diameter of 2.5 mm, which corresponded to a viewing angle of 0.2 deg at the position of the subject's head. The LEDs were powered with current pulses (frequency 150 Hz), and set at a luminance of approximately 2 cd/m^2.

Measurements

Head and eye movements were measured with the magnetic search-coil induction technique (Robinson 1963). Subjects wore a light-

weight helmet (about 150 g), consisting of a narrow strap above the ears, which could be adjusted to fit around the head, and a second strap that ran over the head. A small coil was mounted on the latter. Subjects also wore a scleral search coil on one of their eyes (Collewijn et al. 1975). In the room two orthogonal pairs of 3×3-m^2 square coils were attached to the walls, floor, and ceiling to create the horizontal (30 kHz) and vertical (40 kHz) oscillating magnetic fields that are required for this recording technique. Horizontal and vertical components of head and eye movements were detected by phase-lock amplifiers (Princeton Applied Research, models 128A and 120), low-pass filtered (150 Hz), and sampled at 500 Hz per channel before being stored on disk.

A PC-486 was equipped with the hardware for data acquisition (Metrabyte DAS16), stimulus timing (Data Translation DT2817), and digital control of the LEDs (Philips I2C).

Experimental paradigms

Each experimental session started with three calibration runs to calibrate the eye and head coils (Goossens and Van Opstal 1997b). Before calibration, subjects were asked to keep their head in a comfortable straight-ahead position and adjust a dim red LED mounted at the end of a pliable rod that was attached to the helmet, such that it was aligned with the center LED of the hemisphere. This rod LED was illuminated only during the eye-in-head and head calibration sessions and was extinguished during the actual experiments.

First, eye position in space ("gaze") was determined by calibrating the eye coil. Subjects kept their head still in the straight-ahead position and refixated with their eyes the LED targets on the hemisphere. The targets ($n = 37$) were presented once, in a fixed counterclockwise order, at the center location ($R = 0$), followed by three different eccentricities, $R = [9, 20, 35]$ degrees, and all 12 directions. When subjects fixated the target, they pushed a button to start data acquisition, while keeping their eyes at the target location for ≥1,000 ms.

In the second calibration run, the eye-in-head offset position was measured to account for the potential fixed misalignment of the eye and head coils. To that end, subjects fixated the rod LED to keep their eyes fixed in the head. Subjects were asked to assume the neutral, straight-ahead head position and push a button to start 1,000 ms of data acquisition. This procedure was repeated 10 times.

The third calibration run served to calibrate the head orientation in space. Again, subjects were asked to fixate the rod LED with their eyes and to align it with the same 37 LED targets on the hemisphere as in the eye calibration run. In this way, the eyes remained at the same fixed offset position in the head as in the second calibration run. When the subject pointed to the target, he or she started 1,000 ms of data acquisition by pushing a button.

After the calibration runs were completed, the aluminum rod was removed, and four different localization blocks were performed: *1*) visual single step; *2*) visual–visual double step; *3*) auditory single step, and *4*) visual–auditory double step. Blocks of one modality were always presented together and the single-step block was always presented first. In this paper we will focus on the visual experiments only. Subjects MK, ML, MV, and SP performed only in the visual experiments. The results of the auditory experiments are described in Vliegen et al. (2004). All calibration and experimental sessions were performed in complete darkness.

Visual single-step paradigm

To determine a subject's baseline localization behavior, a single-step experiment was performed. Each trial started with the presentation of a fixation LED. During fixation subjects had their head and eyes approximately aligned. After 800 ms the fixation LED was extinguished and after a 50-ms gap of complete darkness a target LED was flashed for 50 ms at a different location. Subjects were asked to look at the remembered location of the target LED as quickly and accurately as possible. Because stimuli were always well extinguished before the initiation of the eye–head movement, subjects performed under completely open-loop conditions. Moreover, during stimulus presentation the hemisphere and other objects in the room were invisible, so that no exocentric localization cues were available to the subject.

We used two different stimulus configurations. The first consisted of a central fixation target at $[R, \phi] = [0, 0]$ deg and 10 visual target positions with $[R, \phi] = [14, 0]$, $[14, 180]$, $[20, 0]$, $[20, 90]$, $[20, 180]$, $[20, 270]$, $[27, 60]$, $[27, 120]$, $[27, 240]$, or $[27, 300]$ deg. Target locations were selected in random order. One block consisted of 20 trials. Three blocks were run on separate days.

In the second configuration the initial fixation position was at either $[R, \phi] = [20, 90]$ or $[20, 270]$ deg (pseudorandomly chosen with both fixation targets occurring equally often). Visual targets were presented at randomly selected positions within a circle of $R = 35$ deg around the straight-ahead direction, but always ≥10 deg away from the fixation point. A total of 12 trials were presented in one block and at least two blocks were run on separate days. Subjects MK, ML, MV, and SP participated in one block of 96 trials of the second configuration.

Visual–visual double-step paradigm

In the double-step experiment, two visual targets were presented shortly after each other. First, a fixation target was presented for 800 ms. After 50 ms of darkness a first visual target was presented for 50 ms. The second target was also presented for 50 ms, but the timing varied, which resulted in three conditions:

1) Nontriggered (*static*) *condition*, in which the second target was presented after a fixed delay of 50 or 100 ms (first or second target configuration, respectively) after extinction of the first visual target. In this condition, both targets were presented and extinguished before initiation of the first eye–head movement.

2) Head-triggered (*dynamic*) *condition* (first target configuration), in which the second target was triggered as soon as *head* velocity toward the first visual target exceeded 40 deg/s.

3) Gaze-triggered (*dynamic*) *condition* (second target configuration), in which the second target was presented 20 ms after the *gaze* velocity to the first visual stimulus exceeded 60 deg/s.

In both dynamic conditions, the second stimulus was presented while eyes and head were moving. Because in visually evoked gaze shifts the head-movement onset typically follows the eye movement (Goossens and Van Opstal 1997b), the second visual target was typically presented in midflight of the gaze shift for both triggering conditions. Because of the considerable variability in eye–head onset disparities, we also obtained a large range of second target onsets relative to gaze saccade (see RESULTS, e.g., Fig. 5).

As in the single-step experiment, two target configurations were used. To enable direct comparison of the results of the single-step and the double-step experiments, the locations of the first and second visual targets of the double-step paradigm corresponded to the positions of the fixation targets and visual targets of the single-step paradigm. Fixation targets in the double-step experiment were at $[R, \phi] = [35, 0]$ deg or $[35, 180]$ deg in both target configurations. Because in the first configuration the first target was always at $[R, \phi] = [0, 0]$, eight catch trials were included in the experiment to prevent predictive response behavior. In these catch trials the first target was at either $[R, \phi] = [35, 30]$, $[35, 150]$, $[35, 210]$, or $[35, 330]$ deg, and the second target was presented at either $[R, \phi] = [20, 90]$ or $[20, 270]$ deg (pseudorandomly chosen with all positions occurring equally often; for an illustration see Fig. 2 in Vliegen et al. 2004).

Note that in the first target configuration the gaze shift to the first target was always horizontal, whereas in the second target configuration the first gaze shift also had a considerable vertical component.

The double-step block consisted of 48 trials (eight of which were catch trials for the first configuration). Half of the trials were dynamic trials, which were randomly interleaved with the static trials. Three blocks were run on separate days in the first configuration and at least two in the second configuration. Subjects MK, ML, MV, and SP did three to four blocks of 96 trials on one day. In all experimental sessions, subjects were free to move their head and eyes to localize the target. The specific instruction given to the subject was: "*Fixate both visual targets with your eyes as quickly and as accurately as possible.*"

Data analysis

The raw position data from the three calibration sessions were mapped to calibrated azimuth/elevation angles of eye and head position in space by means of two neural networks (for details, see Goossens and Van Opstal 1997b). From the calibrated response data of the localization experiments, head and gaze saccades were identified off-line with a custom-written computer algorithm that detected saccades on the basis of separate onset and offset velocity and acceleration criteria (Goossens and Van Opstal 1997b). Saccade boundaries were visually checked by the experimenter and corrected if needed. Responses with a first-saccade latency <80 ms or >800 ms were discarded from further analysis. All static double-step trials in which the first-saccade latency fell between 80 ms and the second stimulus offset were considered dynamic trials. They were included in the dynamic double-step database, provided mean gaze velocity during stimulus presentation exceeded 50 deg/s.

The coordinates of targets and of calibrated eye and head positions were expressed in a double-pole azimuth-elevation coordinate system, in which the origin coincides with the center of the head (Knudsen and Konishi 1979). In this system, the azimuth angle α is defined as the angle within the horizontal plane with the vertical midsaggital plane, whereas the elevation angle ϵ is defined as the direction within a vertical plane with the horizontal plane through the subject's ears. The straight-ahead direction is defined by $[\alpha, \epsilon] = [0, 0]$ deg. The relation between the $[\alpha, \epsilon]$ coordinates and the polar $[R, \phi]$ coordinates defined by the LED hemisphere (see above) is given by Hofman and Van Opstal (1998).

Statistics

To evaluate to what extent the visuomotor system compensates for intervening eye–head movements, we performed a multiple linear regression on the azimuth and elevation components of the second gaze and head displacement vectors. Regression parameters were determined on the basis of the least-squares error criterion.

The bootstrap method was applied to obtain confidence limits for the optimal fit parameters in the regression analyses. To that end, 1,000 data sets were generated by random selections of data points from the original data. Bootstrapping thus yielded a set of 1,000 different fit parameters. The SDs in these parameters were taken as an estimate for the confidence levels of the parameter values obtained in the original data set (Press et al. 1992). To test whether two fit parameters (GM and HM, Fig. 8, and the parameters for the different models, *Eqs. 4a–4c*) differed significantly, we performed a *t*-test for two independent regression coefficients (Howell 1997).

To determine whether the azimuth-elevation endpoint data for the different conditions were statistically different, we applied the 2D Kolmogorov–Smirnov (KS) test. This test provides a measure (d-statistic) for the maximum distance between the two distributions, for which the significance level (P) of the distributions are the same, can be readily computed (Press et al. 1992). If $P < 0.05$ the two data sets were considered to correspond to different distributions.

The bin width (BW) of histograms (Figs. 4 and 6) was determined by $BW = \text{Range}/\sqrt{n}$, where Range is the difference between the largest and smallest values (excluding the two most extreme points) and n represents the number of included data points.

RESULTS

Figure 3 shows two examples of gaze and head traces of subject MW as a function of time (*top row*), as well as the corresponding spatial trajectories (*bottom row*) for a static (Fig. 3*A*) and a dynamic trial (Fig. 3*B*). Note that in the static condition both targets were indeed presented before gaze and head movement onsets. In the dynamic condition, the second target was presented during the first gaze shift. Typically, gaze starts to move well before the head, which is apparent in both conditions (Fig. 3, *A* and *B*). The dashed square in the spatial plots indicates the location to which responses would be directed if the system would not compensate for the intervening gaze shift. Instead, the eye and head saccades are clearly directed to the actual spatial location of the target.

Figure 4*A* illustrates the spatial trajectories and kinematics of the eye and head movements during the 50 ms that the visual

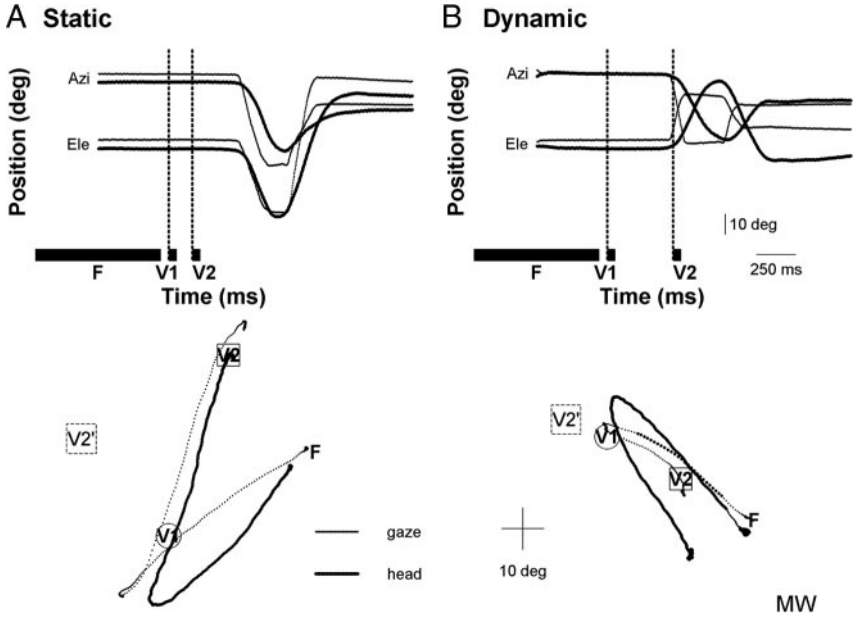

FIG. 3. Temporal and spatial gaze (thin lines) and head (thick lines) traces for one static trial (*A*) and one dynamic trial (*B*) of subject MW. *Top*: temporal traces for gaze and head for both azimuth and elevation. Black bars: target timings for F, V_1, V_2 (target onset shown as vertical dashed lines). *Bottom*: spatial trajectories of head and gaze, and target locations. Time of target presentation is indicated as a change in line thickness. Dashed square: hypothetical response location in case of no compensation for intervening eye–head movements.

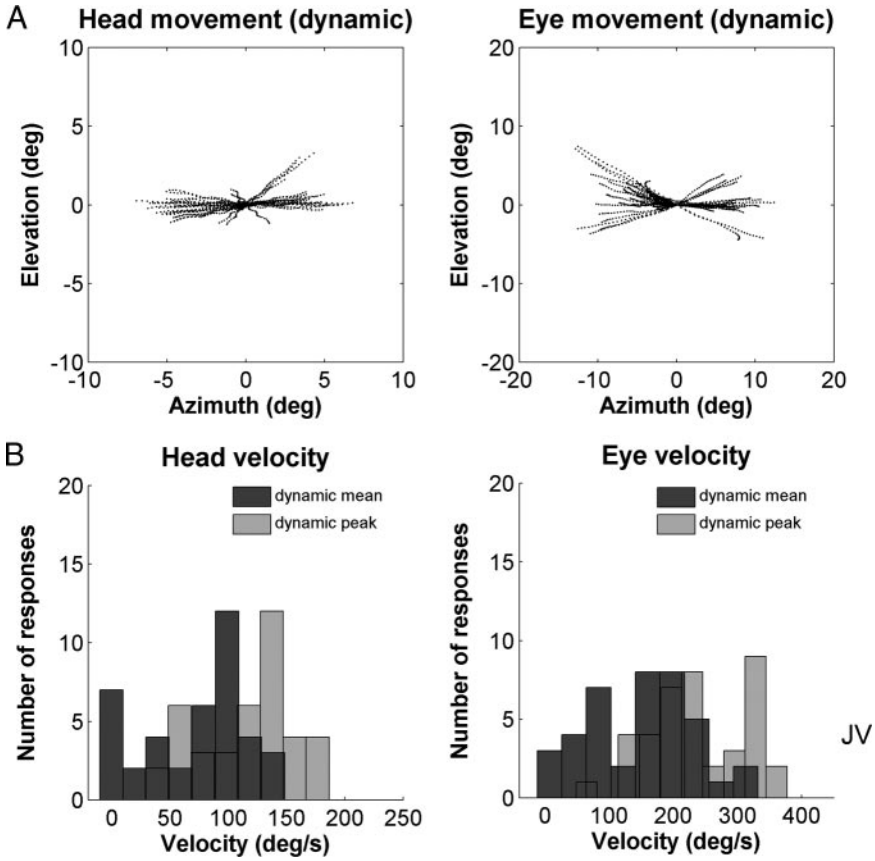

FIG. 4. Head (*left*) and eye (*right*) movement properties during second target presentation. *A*: 2-dimensional head and eye movements during target presentation in the dynamic condition. *B*: histograms of mean and peak head and eye velocity profiles during target presentation. Dark gray histograms: mean velocity during dynamic double steps. Light gray histograms: peak velocity during dynamic double steps. Note large velocity range. Data for all sessions of subject JV.

stimulus was presented in the dynamic double steps, for all experimental sessions of subject JV. Note that the eye movements (and thus the retinal "smearing") can be as large as 15 deg, whereas the head movements are typically somewhat smaller. The latter is explained by the fact that eye velocity is typically higher at the time of stimulus presentation than head velocity. This point is further illustrated in Fig. 4*B*. In the dynamic condition the mean and peak velocities (dark gray and light gray histograms, respectively) show a large trial-to-trial variability. This illustrates the fact that the saccade kinematics varied considerably between trials. Gaze latencies varied between 150 and 668 ms (mean: 258 ms) in the static condition and between 88 and 582 ms (mean: 240 ms) in the dynamic condition. Head latencies varied between 130 and 750 ms (mean: 249 ms) in the static condition and between 122 and 470 ms (mean: 235 ms) in the dynamic condition. Mean amplitude for the second gaze shift was 14 deg, with a maximum of 59 deg, in azimuth and 17 deg with a maximum of 66 deg in elevation. For the head the mean azimuth amplitude was 14 deg, with a maximum of 50 deg, and the mean elevation amplitude was 15 deg with a maximum of 72 deg.

To further demonstrate that the first gaze shift was well under way at the onset of the second target, and thus that ΔG^* differed appreciably from ΔG_1 (see Fig. 2*B*), Fig. 5 shows these two variables plotted against each other, pooled for all subjects. Note that all data points lie clearly below the identity line. Moreover, there is a considerable variability in the $\Delta G^* - \Delta G_1$ differences, indicating that the second target was triggered at various gaze orientations during the first saccade. The two symbols represent the different target configurations. As the head typically lagged the eyes, and had a more variable latency, the ΔG^* values for the first target configuration (head triggered) were typically smaller and more variable than those for the second target configuration (gaze triggered).

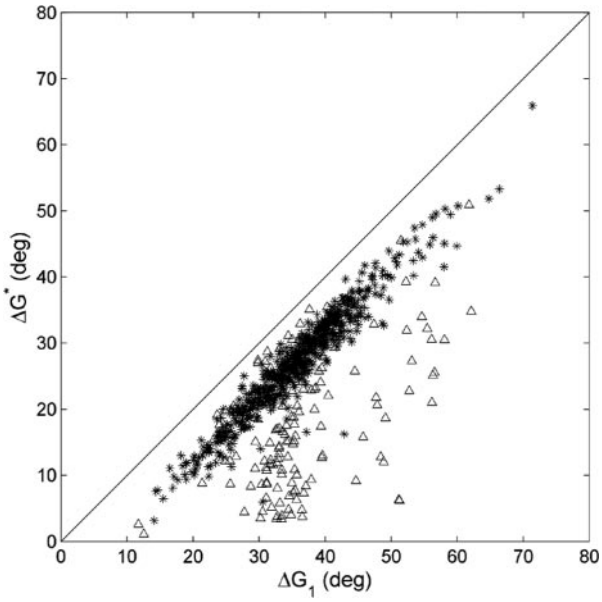

FIG. 5. Partial gaze shift after second target onset (ΔG^*) plotted against the full first gaze shift (ΔG_1). Data pooled for all subjects. Triangles represent data for the first target configuration, in which head movement triggered the second target. Asterisks correspond to the second target configuration, where target triggering was based on eye movement. Note that all data points fall below the identity line and that there is a considerable range of ΔG^* vs. ΔG_1 differences.

In Fig. 6 the 2D distributions of the gaze endpoints to the second target are shown for the static (black filled dots) and the dynamic (gray triangles) double-step condition, as well as for the single-step (open circles) responses for six subjects. In this figure, all target positions (T) were aligned with the origin of the azimuth-elevation coordinate system, and the gaze endpoint coordinates are plotted as an undershoot or overshoot relative to the target location. The black histograms show the distributions of the static double-step data with the means indicated by the black dashed lines. The gray histograms and continuous lines represent the dynamic double-step data. The dotted lines indicate the means of the single-step data. For all subjects, the data cluster around the actual target location, and the means for all three conditions are close together and to the target location. The static and dynamic double-step responses show similar distributions and indeed for seven of nine subjects (JO, JV, MK, ML, MV, SP, TG) the difference between these conditions was not significant. The single-step data distributions, however, had a smaller variance and did differ significantly from both double-step conditions for all subjects (KS test; $P < 0.01$).

From Figs. 3 and 6 it appears that localization responses are directed on average toward the actual spatial location of the visual target for both double-step conditions. To test in a quantitative way to what extent the intervening eye and head movements are accounted for in the second gaze shift, we performed a multiple linear regression analysis on the azimuth and elevation components of the second gaze displacement vector (ΔG_2), which is expressed as a weighted vector sum of the initial target position relative to the eye ($T_{E,0}$), and the first gaze shift (ΔG_1; see also Fig. 1)

$$\Delta G_2 = aT_{E,0} + b\Delta G_1 + c \quad (1)$$

If the second gaze movement would be based only on the initial retinal target location, the slope a should be 1.0 and slope b and offset c should be 0.0. This case corresponds to the right-hand $T_{E,0}$ response vector (dashed) in Fig. 1. However, in case the gaze control system does fully compensate for the intervening gaze shift, the slope b will be exactly −1.0 (the response then corresponds to arrow $T_{E,2}$ in Fig. 1). Figure 7*A* shows the values of the actual regression coefficients for the static and dynamic stimulation conditions and for the horizontal and vertical response components (pooled data of all subjects and sessions). Apparently, the gaze control system does account for the previous movement because coefficient a was found to be around 1.0 and b close to −1.0 for all conditions. The offsets (c) were close to 0 deg and are not shown.

We performed a similar regression on the second head displacement (ΔH_2), to check whether the head also made goal-directed movements. Thus ΔH_2 was described as a function of the initial target position relative to the eye ($T_{E,0}$), the first gaze shift (ΔG_1), and the eye-in-head offset position at the start of the second gaze shift (E_1)

$$\Delta H_2 = aT_{E,0} + b\Delta G_1 + cE_1 + d \quad (2)$$

If the head would move toward the spatial target position, parameters a and c should be 1.0, b should be −1.0, and d should be 0.0 (corresponding to response arrow $T_{H,2}$ in Fig. 1; see also the

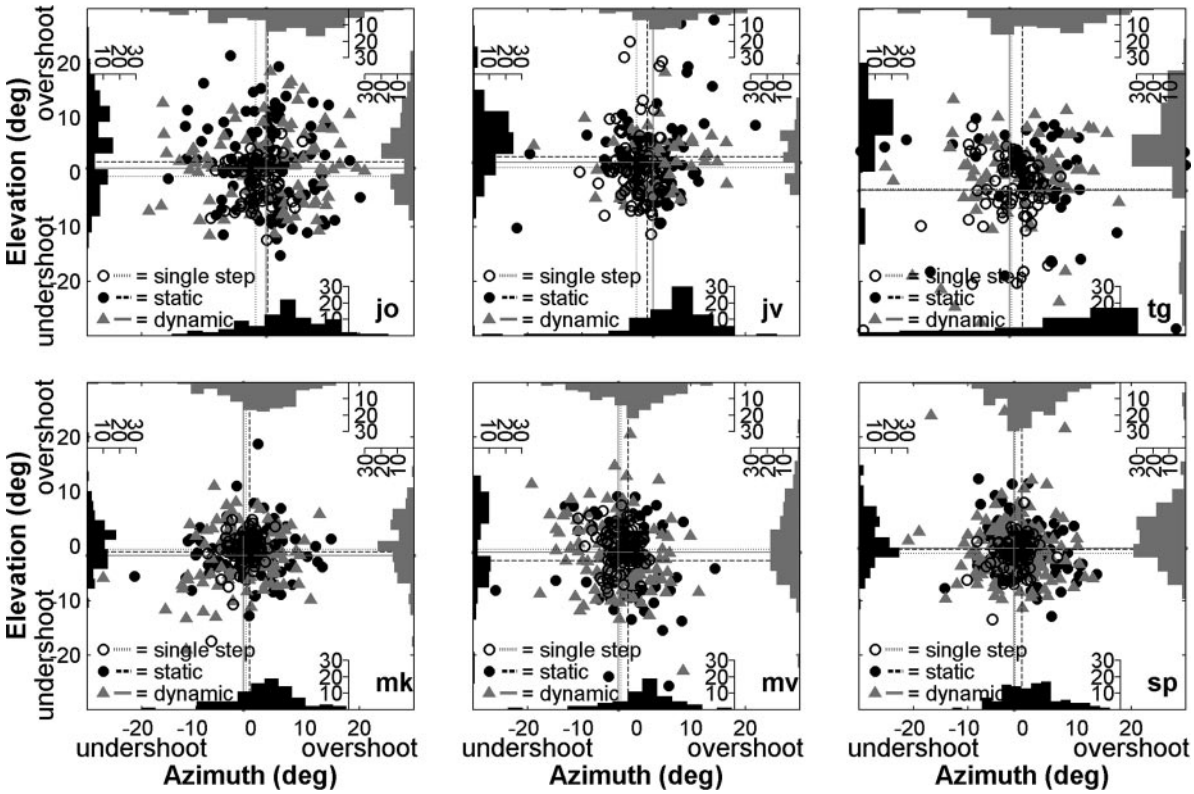

FIG. 6. Endpoints of the second gaze saccades for both double-step conditions (static data: filled black dots; dynamic data: gray triangles) and single steps (open circles) for 6 subjects. All second target positions (T) are aligned with the origin and localization responses are shown as undershoots or overshoots relative to target position. Distributions of the double-step responses, together with their means, are shown as black histograms and a black dashed line for the static condition and gray histograms and a gray solid line for the dynamic condition. Single-step means are indicated by the dotted lines.

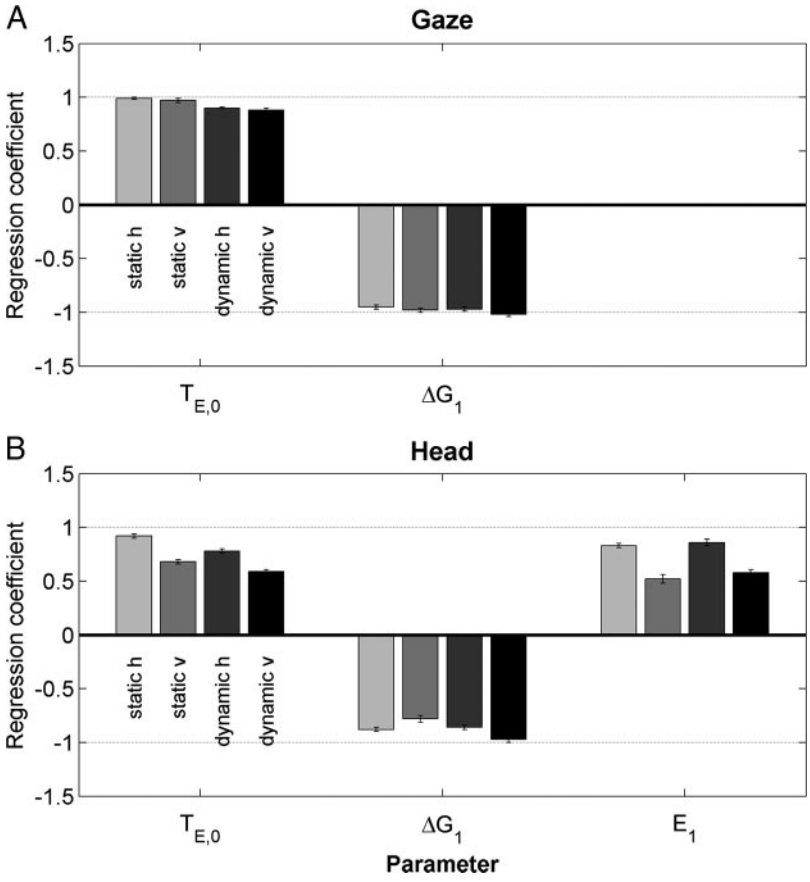

FIG. 7. *A*: regression coefficients of *Eq. 1* for second gaze shifts (ΔG_2), on pooled data of all subjects and sessions. *B*: regression coefficients of *Eq. 2* for second head shifts (ΔH_2). Different gray-colored bars indicate different directions (azimuth, elevation) and double-step conditions (static, dynamic). Error bars indicate SD. Dotted lines at +1.0 and −1.0 correspond to the ideal values for full compensation.

legend of Fig. 1). The results are summarized in Fig. 7*B*. For all conditions a was found to be fairly close to 1.0 and b close to −1.0. The value of c differed between conditions, but was always significantly different from zero and positive. Note that subjects did not receive any specific instructions about their head movements. As a result, the eye position coefficient varied across subjects and sessions, and was less than the ideal value. The offsets (d) were around zero and are not shown.

If eyes and head are both free to move, it is not trivial that both move toward the target, especially if they are not aligned at the onset of the gaze shift. In that case they have to move in different directions to reach the target (e.g., Fig. 1). For that to happen, the respective motor commands need to be transformed into oculocentric and craniocentric coordinates, respectively. Alternatively, eyes and head could both be driven by a common signal, like the gaze motor error, as has been proposed for the common-gaze control model (Galiana and Guitton 1992; Guitton 1992; Vidal et al. 1982). To further quantify whether the eyes and head were indeed driven by a common error signal, or by signals expressed in their own reference frame, we performed a normalized multiple regression on the data in which the second gaze movement ΔG_2 and head movement ΔH_2 were each described as a function of both the gaze motor error (GM) and the head motor error (HM) at movement onset

$$\Delta G_2' = pGM' + qHM' \quad (3a)$$

$$\Delta H_2' = pGM' + qHM' \quad (3b)$$

In *Eqs. 3a* and *3b* the GM and HM vectors were determined as the difference between the spatial location of the second target and the gaze and head position in space at the second gaze shift onset. These variables were then transformed into their (dimensionless) z-scores: $x' = (x - \mu_x)/\sigma_x$, where μ_x is the mean of variable x and σ_x is its variance. In this way, the variables are dimensionless, and p and q are the (dimensionless) partial correlation coefficients for GM and HM, respectively. If $p > q$, the eye (or head) is driven predominantly by an oculocentric gaze-error signal. If $q > p$, the eye (or head) rather follows the head-centered motor error signal. In case $p > q$ (or $p < q$), for both equations, eye and head are driven by the same error signal. To allow for a meaningful dissociation of the oculocentric and craniocentric reference frames, we incorporated trials only for which the absolute azimuth or elevation component of eye-in-head position exceeded 10 deg, and the directional angle between the head and gaze motor-error vectors was ≥15 deg (we thus obtained 200–270 trials, depending on condition).

Figure 8 shows the regression coefficients on the pooled data from all subjects for all conditions. Eye-in-space (Fig. 8*A*) is clearly driven by the eye motor error because the coefficients for gaze motor error are much larger than those for head motor error (*t*-test: for all conditions $P < 0.001$). Conversely, the head movements (Fig. 8*B*) appear to be driven by the HM. The difference between p and q was significant for the horizontal, but not for the vertical conditions ($P < 0.001$).

In the INTRODUCTION we described three different models to predict the second gaze shift in a double-step experiment. All models account for intervening eye–head movements, but they

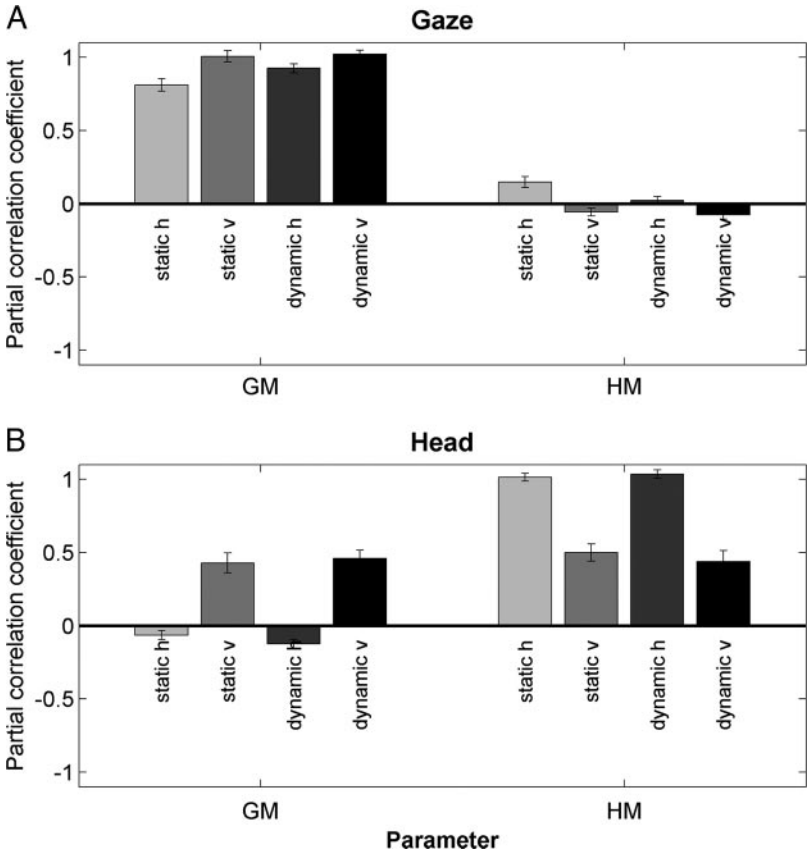

FIG. 8. Partial correlation coefficients for the regression on second gaze saccade (ΔG_2) (*A*) and second head saccade (ΔH_2) (*B*), which are described as a function of gaze-motor error and head-motor error (*Eqs. 3a* and *3b*). Data pooled across subjects and sessions. Same format as in Fig. 7.

differ in the type of information used to update the initial retinotopic target location ($T_{E,0}$). According to the predictive remapping models, information about planned eye–head movements is used; this could be based either on purely visual information [visual predictive (VP)] or on the actual planned movement [motor predictive (MP)]. The dynamic feedback model (FB) states that target position is updated based on continuous information of eye and head movements. The three different models can thus be quantified by

$$\Delta G_{VP} = aT_{E,0} + bFV_1 + c \quad (4a)$$

$$\Delta G_{MP} = aT_{E,0} + b\Delta G_1 + c \quad (4b)$$

$$\Delta G_{FB} = aT_{E,0} + b\Delta G^* + c \quad (4c)$$

where FV_1 is the retinal error of the first target, ΔG_1 is the first saccade vector, and ΔG^* is the partial first gaze shift after stimulus presentation. In the static double step, where both targets are presented before the eye–head movement onsets, the motor-predictive model (*Eq. 4b*) makes the same prediction as the dynamic feedback model (*Eq. 4c*). To calculate the predictions for these different models, we substituted the ideal values of a = 1.0, b = −1.0, and c = 0.0 in *Eqs. 4a–4c*. For the static double steps we thus found that the MP/FB models outperformed the VP model for both the horizontal (R^2: 0.89 vs. 0.70, respectively) and vertical (R^2: 0.91 vs. 0.80, respectively) response components (data not shown). This result therefore demonstrates that the visuomotor system accounts for the actual intervening gaze shift, ΔG_1, rather than for the initial retinal error (FV_1; see Fig. 2).

However, for the dynamic condition the predictions of the MP and FB models are dissociated because ΔG_1 and ΔG^* are different (see Fig. 5). Figure 9 shows the predictions of the three different models plotted against the actually measured second gaze shift for the dynamic double steps. Figure 9*A* shows the data for the head-triggered paradigm. As is apparent from Fig. 5, the differences between ΔG_1 and ΔG^* are largest and more variable for this experiment, which is a key point in discriminating between the predictive remapping models and the dynamic feedback model. Here, we show only the horizontal components of the second gaze shifts because in this paradigm the initial gaze shift was always purely horizontal (see METHODS). In Fig. 9*B* all data are pooled across subjects and sessions and are shown for both horizontal and vertical response components. In all cases, the predictions for the dynamic feedback model outperform the predictive remapping models. This is most strongly demonstrated for the head-triggered data in Fig. 9*A*.

We also performed linear fits on the measured ΔG_2 for all three models, given in *Eqs. 4a–4c* to determine the actual regression coefficients. We applied these fits on the data of the dynamic double steps, both for the head-triggered data, separately, and for all data pooled, to quantify the dissociation between the predictive remapping models and the dynamic feedback model. The optimal fit parameters are given in Table 1, together with the R^2 values of the fits. If a model provides a good prediction of the measured ΔG_2, not only should R^2 be 1, but also the parameter values should be close to the ideal values of a = 1.0, b = −1.0, and c = 0.0 (see Figs. 1 and 2). The two predictive remapping models give a rather good prediction, with R^2 values of 0.77 or higher, although their optimal parameter values clearly differ from 1.0 and −1.0. The dynamic feedback model however, yields parameter values

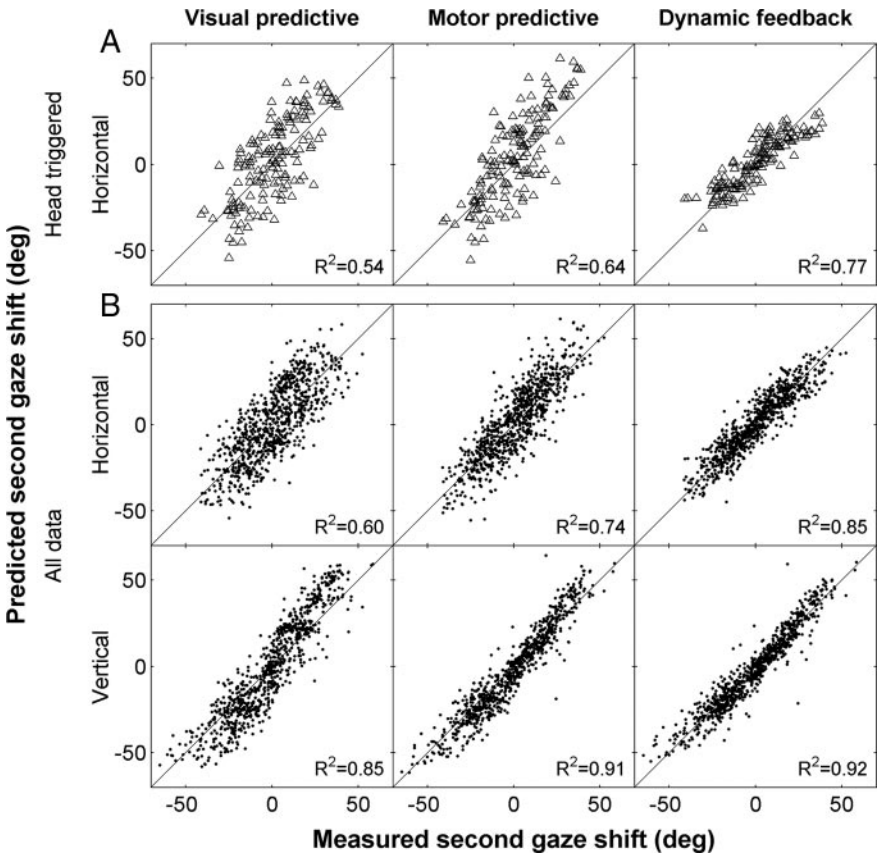

FIG. 9. Predictions for the second gaze shift (ΔG_2) for 3 different models (columns) as a function of the measured second gaze shift. *A*: data for the dynamic condition of the head-triggered paradigm (horizontal data only, pooled across subjects). *B*: horizontal and vertical response components for all data, pooled across subjects and sessions. If a model would predict ΔG_2 perfectly, the data would fall on the identity line and R^2 would be 1. R^2 values are given in the *bottom right corner* of all panels. In all cases, the dynamic feedback model provides the best prediction for the data.

that are close to these ideal values, and R^2 values that are closest to 1.0. As expected, the difference is largest for the head-triggered data. The a and b values of the dynamic feedback model are significantly different from both predictive models for the horizontal and vertical response components ($P < 0.001$ for all conditions, except for the a values for all data in the vertical condition).

Accuracy around saccade onset

In contrast to the accurate localization responses found by Hallett and Lightstone (1976) in their dynamic double steps, Dassonville et al. (1995) reported systematic errors when short-duration (2-ms) visual targets were presented near saccade onset (for a review also see Schlag and Schlag-Rey 2002). To test whether this discrepancy in results might have been caused by the presence or absence of allocentric localization cues (e.g., the difference vector between the target locations on the retina), Dassonville et al. (1995) systematically varied the dark gap between the two targets between 45 and 495 ms. However, only part of the discrepancy with data reported by Hallett and Lightstone (1976) could be explained by a potential allocentric cue because errors diminished only slightly for the shortest gaps. Also Honda (1990, 1991) obtained systematic localization errors for stimuli presented before saccade onset, like Dassonville et al. (1995), but he also reported errors in the opposite direction after saccade onset. In our experiments a considerable variation also arose in the duration of the dark period between the first and second visual targets that ranged from 50 to 590 ms (nontriggered: 50 ms; triggered: 80–590 ms). In Fig. 10*A*, we have therefore plotted our data in the same way as Dassonville et al. (1995; their Fig. 2), with mean azimuth localization error plotted against stimulus onset relative to gaze shift onset. Localization error is plotted relative to the direction of the first gaze shift, with positive values indicating an error in the same direction as the first gaze shift. The

TABLE 1. *Fit parameters of dynamic double steps for the three models*

		a		b		c, deg		R^2	
Model	Condition	$n = 153$	$n = 796$	$n = 153$	$n = 796$	$n = 153$	$n = 796$	$n = 153$	$n = 796$
VP	Dyn. hor.	0.72	0.82	−0.55	−0.61	−1.09	−0.06	0.77	0.85
	Dyn. ver.	—	0.87	—	−0.55	—	−0.70	—	0.93
MP	Dyn. hor.	0.77	0.85	−0.57	−0.67	−2.15	−0.65	0.85	0.91
	Dyn. ver.	—	0.87	—	−0.78	—	0.86	—	0.95
FB	Dyn. hor.	1.00	0.90	−1.24	−0.97	−0.87	−0.44	0.92	0.92
	Dyn. ver.	—	0.88	—	−1.02	—	0.45	—	0.96
Ideal		1		−1		0		1	

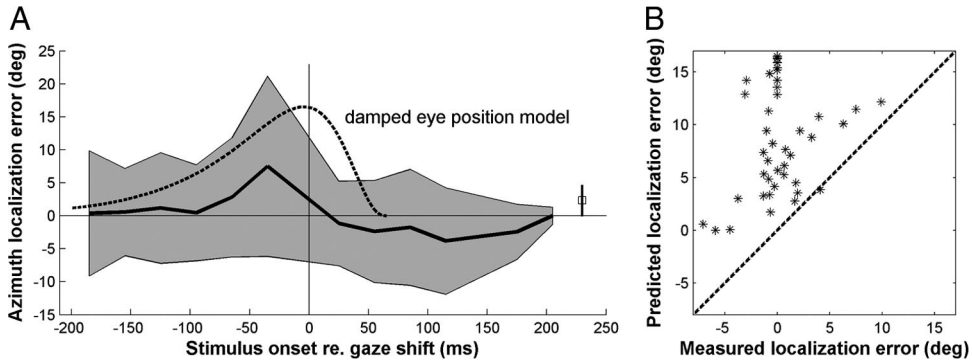

FIG. 10. *A*: mean gaze localization error (azimuth) of the second target as a function of second stimulus onset relative to saccade onset (black line), together with SDs (gray area). Negative values of stimulus onset indicate trials where the second stimulus is presented before gaze shift onset; for positive values the stimulus is presented after gaze shift onset. Localization error is plotted relative to the direction of the first gaze shift, with positive values indicating an error in the same direction as the first gaze shift. Mean single-step localization error (with SD) is shown as an open square at an onset value of 230 ms. Dashed line: estimate of the prediction of a damped eye position model (Schlag et al. 1989), based on the results of Dassonville et al. (1995). *B*: predicted localization error according to the damped eye position model vs. the measured localization error. Note that all points lie above the unity line.

dashed line is the prediction of the damped eye-position model of Dassonville et al. (1995) and Schlag et al. (1989; time constant 65 ms) for a 35 deg horizontal gaze shift. Figure 10*B* plots the measured and the predicted errors against each other. In contrast to Dassonville et al. (1995) and Honda (1990, 1991), but in line with Hallett and Lightstone (1976), we did not obtain a large systematic increase in the localization error around gaze-shift onset in the direction of the first saccade.

DISCUSSION

Summary

Our results show that visual localization remains accurate for the three experimental paradigms in this study: single steps, static double steps, and dynamic double steps. Despite the fundamentally different sensorimotor transformations, on average responses were directed toward the actual spatial location of the second target for all three conditions (Figs. 3 and 6). Although gaze endpoint variability for double steps is higher than that for single steps, we did not obtain systematic localization errors (Fig. 6). Gaze shifts remained accurate for dynamic double steps, despite the high intertrial variability of eye and head displacements and kinematics during target presentation (Fig. 4). We conclude that intervening eye–head gaze shifts have not been incorporated by a preprogramming strategy (neither based on visual input, as in the visual-predictive model, nor by the intended gaze shift, as in the motor-predictive model). Instead, we propose that the gaze control system updates target locations dynamically, through continuous feedback about ongoing eye and head movements.

Related studies

Mays and Sparks (1980) and Sparks and Mays (1983) showed that monkeys redirect their gaze to previously flashed visual targets, even after microstimulation in the SC induced an intervening saccade that was not planned by the animal. Schlag-Rey et al. (1989) interrupted spontaneous and visually elicited saccades by SC microstimulation and found that the saccade resumed its trajectory toward a new saccade goal imposed by the induced perturbation. The authors conjectured that microstimulation created a "phosphene " that served as a new goal for the visuomotor system. Such goal-directed responses were not obtained when stimulation was applied to the SC motor layers.

In contrast to Dassonville et al. (1995), we did not observe systematic localization errors when the target was flashed around gaze-shift onset (Fig. 10). It is not immediately clear which factors underlie this apparent discrepancy in results because their stimulus conditions closely resembled those in this study (i.e., complete darkness and absence of allocentric cues), although our stimuli had a longer duration (50 vs. 2 ms) and they were brighter (2 cd/m^2 vs. 15 mcd/m^2). As a result, our stimuli induced a larger and clearer dynamic retinal "smearing, " which may have provided partial information about the ongoing gaze shift (Fig. 4). Indeed, Festinger and Holtzman (1978) demonstrated a slight benefit on saccade accuracy when saccadelike retinal smearing was applied to the stimulus during the entire saccade. Yet, retinal smearing alone cannot explain the accurate responses in our experiments because considerable portions of the gaze shifts remained in complete darkness after target offset.

Although our stimuli were much brighter than those reported by Dassonville et al. (1995), they did not induce a noticeable retinal afterimage, nor did they provide additional visual cues through spurious reflections on surfaces in the environment. Even if there would be visual cues, visual landmarks are subjected to a strong perceptual deformation around a saccadic event, leading to systematic perceptual localization errors (Bremmer and Krekelberg 2003; Lappe et al. 2000; Ross et al. 1997). Yet, such systematic localization errors were not obtained in our study either (Fig. 10). Moreover, as illustrated in Fig. 2, retinal events alone cannot explain spatially accurate behavior because this requires adequate use of motor signals.

If gaze control relied on a sluggish, low-pass–filtered eye (and possibly head) position signal, like Schlag et al. (1989) and Dassonville et al. (1995) propose, it is not obvious why such a (motor) effect disappears for brighter and longer-duration stimuli. Indeed, our recent report that gaze shifts remain accurate also when the second stimulus is a brief *auditory* target (Vliegen et al. 2004) cannot be attributed to visual factors.

A final difference with earlier studies is that our subjects were free to move eyes and head. Perhaps these more natural

orienting responses may have enabled the system to better use available egocentric movement cues.

In an attempt to unite the apparently discrepant data sets, we conjecture that gaze control and perception may depend on the strength (or reliability) of the available sensory and motor cues. Thus the integrity of the motor feedback signals could also depend on the signal-to-noise ratio of the sensory input. For very weak visual stimuli the system's feedback pathway might thus be only partially engaged, resulting in an apparently lagged eye-position signal and error patterns along the saccade direction. For more salient sensory inputs, eye and head positions could be fully incorporated in the transformations.

Perception versus action

Despite our conclusion that predictive remapping cannot account for spatially accurate performance in dynamic double steps, there is ample neurophysiological evidence that such a mechanism is engaged in visuomotor behavior (Colby et al. 1995; Duhamel et al. 1992; Umeno and Goldberg 1997; Walker et al. 1995). Possibly, predictive information about impending saccades primarily subserves perceptual stability of the visual environment across saccades, rather than the coordination of accurate saccade sequences (action; Bremmer and Krekelberg 2003; Burr et al. 2001). Such an interpretation would also be consistent with saccadic adaptation experiments. In that paradigm, the saccade triggers the stimulus to rapidly jump toward a new location. Initially, the primary saccade is consistently followed by a corrective saccade to the new target location. However, during the course of many repetitions, the saccade gradually incorporates the future target jump, to eventually land on the target without the need for corrective responses. Neurophysiological evidence has indicated that adaptation acts downstream from the motor SC (Edelman and Goldberg 2002; Frens and Van Opstal 1997). Recently, Bahcall and Kowler (1999) found that perceptual localization of the target was affected by adaptation, indicating that perception did not have access to information about the adapted saccade. Rather, perception appeared to use a signal about the *intended* saccade for the initial retinal error, irrespective of the intrasaccadic target jump. More recently, however, Awater et al. (2005) challenged this conclusion. In contrast, secondary saccades in static double steps compensate for the adapted first saccade (Tanaka 2003), which suggests that in the double-step paradigm the visuomotor system *does* have access to the actual saccade commands. These studies, together with the present data, therefore support the notion that separate neural pathways are involved in spatial perception, and in spatially accurate movement planning, or action (Burr et al. 2001).

Model implications

So far, we have not made explicit which feedback signals may be used in target updating. Here, we confront the concepts of *displacement* feedback versus *position* feedback (see INTRODUCTION). Although these concepts were initially developed for the oculomotor system, and primarily based on static double-step results, we here apply these ideas to dynamic eye–head gaze control.

According to displacement models, the visuomotor system keeps the target in an *oculocentric* reference frame, which is updated by an ongoing gaze *displacement* signal to generate a spatially accurate dynamic gaze motor error

$$\Delta G_2(t) = T_{E,0} - \Delta G_1(t) \quad (5)$$

Alternatively, in position models the retinal target location $T_{E,0}$ is first transformed into an *absolute* reference frame (e.g., a world-reference frame), by adding gaze position at stimulus onset G_0

$$T_W = T_{E,0} + G_0 \quad (6)$$

This target location is then updated to gaze motor error by subtracting the current gaze position G(t)

$$\Delta G_2(t) = T_W - G(t) \quad (7)$$

Note that both models (*Eqs. 5* and *7*) yield identical results, but the position model requires an additional transformation stage (*Eq. 6*). So far, neurophysiological evidence has favored the displacement scheme. For example, cells in the primate FEF have discharges that relate to the three signals figuring in *Eq. 5* (Goldberg and Bruce 1990). Recently, Sommer and Wurtz (2002, 2004) provided evidence that the mediodorsal thalamus mediates a signal with information about the impending collicular eye-displacement command to the FEF, which might be used to update the target in a double-step paradigm. Conversely, an explicit neural code of the target in a world-fixed reference frame has not been found.

The neurophysiological evidence notwithstanding, here we argue that our dynamic double-step results are hard to reconcile with a displacement scheme. Figure 11 illustrates the problem for the eye-in-space movement only, ignoring the head movement for simplicity. Suppose that the eye makes a gaze shift ΔG_1 toward the first visual target T_1, and that T_2 is flashed in midflight, when gaze position is G*. According to the position model, the target is first updated to an extraretinal (world) reference frame by adding gaze position to the retinal target location: $T_{W*} = T_{E*} + G*$. At the end of the saccade, the gaze position is G_1 and the gaze motor error is: $\Delta G_2 = T_{W*} - G_1$ (*Eq. 7*). A gaze-displacement scheme needs only to subtract the eye movement after the second target onset from the retinal error to yield the gaze motor error at saccade offset: $\Delta G_2 = T_{E*} - \Delta G*$ (*Eq. 5*).

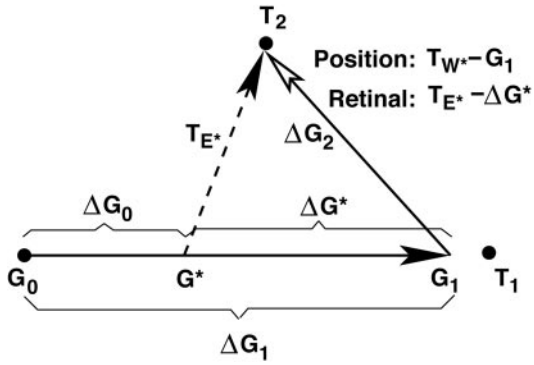

FIG. 11. Coordinate transformations for a visual target at T_2, presented in midflight of a saccadic gaze shift (gaze-displacement vector, ΔG_1) to visual target T_1. Head movements are omitted for simplicity. G_0, gaze position at the start of the trial; ΔG_0, gaze displacement up to second target onset; T_{E*}, target in retinal coordinates; G*, gaze position at second target onset; T_{W*}, target in world coordinates; G_1, gaze position at saccade offset. ΔG_2, gaze motor error at saccade offset; $\Delta G*$, gaze displacement after second target onset. See text for explanation.

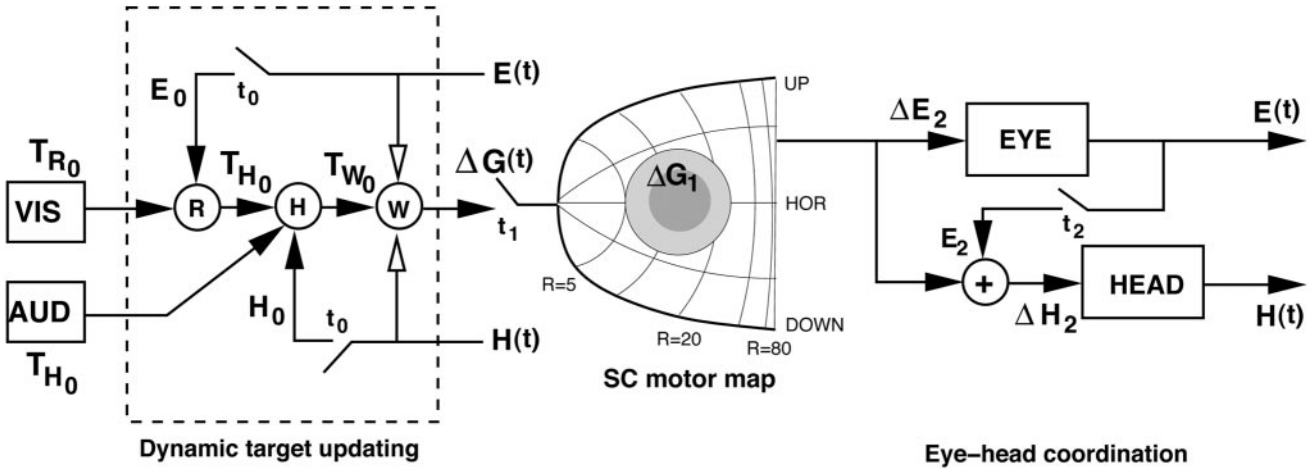

FIG. 12. Model for dynamic eye–head coordination to auditory and visual targets. Dynamic updating pathway builds a representation of auditory and visual targets in a world reference frame (T_{W_0}), by combining the retinal error (T_{R_0}) with eye (E_0) and head position (H_0) at second target onset (time t_0). Head-centered auditory input (T_{H_0}) is combined with head position only. Remembered target location is continuously combined with current eye [E(t)] and head [H(t)] position, yielding a dynamic target estimate in oculocentric coordinates [G(t)]. When the gaze shift is selected (time t_1), a local population of cells in the SC motor map is activated, representing the desired gaze displacement vector (ΔG_1). This collicular signal drives eye and head motor systems at time t_2. Local feedback circuits downstream from the SC ensure that eyes and head are driven in their own motor frames: ΔE_2 and ΔH_2, respectively. Details of the latter circuits are omitted for clarity. Filled arrowheads: excitatory projections; open arrowheads: inhibitory projections. E_2: eye position at gaze shift onset.

However, the apparent simplicity of this latter model to explain static double-step behavior now encounters a serious difficulty. Given the visual delays in the system, and the need to restart the computation of gaze displacement in midflight at second target onset (while discarding the gaze displacement so far, ΔG_0), it is not at all obvious how the visuomotor system may attain access to ΔG^*. To generate such a signal would require either a new resettable integrator or resetting/restarting the only resettable integrator. Recent studies suggest that this process may involve a leaky process that takes ≥50 ms (Nichols and Sparks 1995).

In the position scheme, a potential delay is not immediately fatal because a neural estimate of eye position could be readily available from the oculomotor brain stem and, even if the computation of T_{W^*} might take some time, it could be finished during the continuation of the movement.

Note also that for saccades to (head-fixed) auditory targets, a signal related to eye *position*, not to eye displacement, is needed to construct the eye motor error (Jay and Sparks 1984). We therefore propose that the updating of target locations relies on instantaneous absolute positions, rather than on relative displacements.

Figure 12 provides a conceptual model for the different stages within the gaze control system that transforms auditory and visual targets into a world-reference frame, and subsequently into a dynamic oculocentric gaze-displacement signal. For a visual stimulus, retinal error is first combined with eye (E_0) and head (H_0) position at second target onset (t_0) to construct an extraretinal target representation (T_{W_0}). For auditory localization, head position (H_0) suffices for this transformation. In line with the dynamic double step results, current eye and head positions are combined with this memorized target representation, yielding a dynamic estimate of the target in eye-centered coordinates, $\Delta G(t)$. If a saccade is planned to the target (at t_1), a fixed, local population of cells in the SC motor map is recruited that represents the desired gaze displacement, ΔG_1. This signal drives the eye and head motor systems in their own motor frames, $\Delta E_2 = \Delta G_1$, and ΔH_2, respectively (e.g., Fig. 8). To compute the latter signal, eye-in-head position E_2, at movement initiation (t_2), is required.

Neurophysiological correlates

Our scheme proposes that the dynamic transformation of target location occurs upstream from the motor SC. A potential candidate for these transformations may be the posterior parietal cortex (PPC; Andersen 1997). Although individual cells in PPC appear to possess oculocentric auditory and visual receptive fields, rather than receptive fields in world coordinates (Stricanne et al. 1996), many PPC cells have also been shown to be modulated by eye and head position signals (Snyder et al. 1998). In this way, PPC cells are better characterized by so-called gain fields, than by a purely visual receptive field. Simulations have indicated that a distributed population of cells with gain field modulations could simultaneously represent the target in retinotopic, craniocentric, and in world coordinates (Van Opstal and Hepp 1995; Xing and Andersen 2001; Zipser and Andersen 1988). Interestingly, PPC cells have also been shown to be involved in predictive remapping (Duhamel et al. 1992). The PPC could therefore play a crucial role in both the perception of, and the actions in, sensorimotor space. At present it is unclear whether cells displaying gain fields and cells showing predictive remapping belong to the same population, or to different subpopulations.

ACKNOWLEDGMENTS

We thank G. Van Lingen, H. Kleijnen, G. Windau, and T. Van Dreumel for valuable technical assistance and J. Goossens for helpful discussions and suggestions.

GRANTS

This research was supported by the Radboud University Nijmegen (A. J. Van Opstal and T. J. Van Grootel) and the Netherlands Organization for Scientific Research (section Maatschappij en Geesteswetenschappen, project 410-20-301; J. Vliegen).

REFERENCES

Andersen RA. Multimodal integration for the representation of space in the posterior parietal cortex. *Philos Trans R Soc Lond B Biol Sci* 352: 1421–1428, 1997.

Awater H, Burr D, Lappe M, Morrone MC, and Goldberg ME. Effect of saccadic adaptation on localization of visual targets. *J Neurophysiol* 93: 3605–3614, 2005.

Bahcall DO and Kowler E. Illusory shifts in visual direction accompany adaptation of saccadic eye movements. *Nature* 400: 864–866, 1999.

Becker W and Jürgens R. An analysis of the saccadic system by means of double-step stimuli. *Vision Res* 19: 967–983, 1979.

Bremmer F and Krekelberg B. Seeing and acting at the same time: challenges for brain (and) research. *Neuron* 38: 367–370, 2003.

Burr DC, Morrone MC, and Ross J. Separate visual representations for perception and action revealed by saccadic eye movements. *Curr Biol* 11: 798–802, 2001.

Colby CL, Duhamel JR, and Goldberg ME. Oculocentric spatial representation in parietal cortex. *Cereb Cortex* 5: 470–481, 1995.

Collewijn H, Van der Mark F, and Jansen TC. Precise recording of human eye movements. *Vision Res* 15: 447–450, 1975.

Dassonville P, Schlag J, and Schlag-Rey M. Oculomotor localization relies on a damped representation of saccadic eye displacement in human and nonhuman primates. *Vis Neurosci* 9: 261–269, 1992.

Dassonville P, Schlag J, and Schlag-Rey M. The use of egocentric and exocentric location cues in saccadic programming. *Vision Res* 35: 2191–2199, 1995.

Duhamel JR, Colby CL, and Goldberg ME. The updating of the representation of visual space in parietal cortex by intended eye movements. *Science* 255: 90–92, 1992.

Edelman JA and Goldberg ME. Effect of short-term saccadic adaptation on saccades evoked by electrical stimulation in the primate superior colliculus. *J Neurophysiol* 87: 1915–1923, 2002.

Festinger L and Holtzman JD. Retinal image smear as a source of information about magnitude of eye movement. *J Exp Psychol Hum Percept Perform* 4: 573–585, 1978.

Frens MA and Van Opstal AJ. Role of monkey superior colliculus in saccadic short term adapation. *Brain Res Bull* 43: 473–484, 1997.

Galiana HL and Guitton D. Central organization and modeling of eye–head coordination during orienting gaze shifts. *Ann NY Acad Sci* 656: 452–471, 1992.

Goldberg ME and Bruce CJ. Primate frontal eye fields. III. Maintenance of a spatially accurate saccade signal. *J Neurophysiol* 64: 489–508, 1990.

Goossens HHLM and Van Opstal AJ. Local feedback signals are not distorted by prior eye movements: evidence from visually evoked double saccades. *J Neurophysiol* 78: 533–538, 1997a.

Goossens HHLM and Van Opstal AJ. Human eye–head coordination in two dimensions under different sensorimotor conditions. *Exp Brain Res* 114: 542–560, 1997b.

Guitton D. Control of eye–head coordination during orienting gaze shifts. *Trends Neurosci* 15: 174–179, 1992.

Hallett PE and Lightstone AD. Saccadic eye movements towards stimuli triggered by prior saccades. *Vision Res* 16: 99–106, 1976.

Hofman PM and Van Opstal AJ. Spectro-temporal factors in two-dimensional human sound localization. *J Acoust Soc Am* 103: 2634–2648, 1998.

Honda H. Eye movements to a visual stimulus flashed before, during, or after a saccade. In: *Attention and Performance*, edited by Jeannerod M. Hillsdale, NJ: Erlbaum, 1990, vol. 13, p. 567–582.

Honda H. The time courses of visual mislocalization and of extraretinal eye position signals at the time of vertical saccades. *Vision Res* 31: 1915–1921, 1991.

Howell DC. *Statistical Methods for Psychology.* Belmont, CA: Duxbury Press, 1997.

Jay MF and Sparks DL. Auditory receptive fields in primate superior colliculus shift with changes in eye position. *Nature* 309: 345–347, 1984.

Jürgens R, Becker W, and Kornhuber HH. Natural and drug-induced variations of velocity and duration of human saccadic eye movements: evidence for a control of the neural pulse generator by local feedback. *Biol Cybern* 39: 87–96, 1981.

Knudsen EI and Konishi M. Mechanisms of sound localization in the barn owl (*Tyto alba*). *J Comp Physiol* 133: 13–21, 1979.

Kopinska A and Harris LR. Spatial representation in body coordinates: evidence from errors in remembering positions of visual and auditory targets after active eye, head, and body movements. *Can J Exp Psychol* 57: 23–37, 2003.

Lappe M, Awater H, and Krekelberg B. Postsaccadic visual references generate presaccadic compression of space. *Nature* 403: 892–895, 2000.

Mays LE and Sparks DL. Saccades are spatially, not retinocentrically, coded. *Science* 208: 1163–1165, 1980.

Nichols MJ and Sparks DL. Nonstationary properties of the saccadic system: new constraints on models of saccadic control. *J Neurophysiol* 73: 431–435, 1995.

Ottes FP, Van Gisbergen JAM, and Eggermont JJ. Metrics of saccade responses to visual double stimuli: two different modes. *Vision Res* 24: 1169–1179, 1984.

Press W, Teukolsky S, Vetterling W, and Flannery B. *Numerical Recipes in C.* Cambridge, UK: Cambridge Univ. Press, 1992.

Robinson DA. A method of measuring eye movement using a scleral search coil in a magnetic field. *IEEE Trans BME* 10: 137–145, 1963.

Robinson DA. Eye-movements evoked by collicular stimulation in alert monkey. *Vision Res* 12: 1795–1808, 1972.

Ron S, Berthoz A, and Gur S. Saccade-vestibulo-ocular reflex co-operation and eye-head uncoupling during orientation to flashed target. *J Physiol* 464: 595–611, 1993.

Ron S, Berthoz A, and Gur S. Model of coupled or dissociated eye-head coordination. *J Vestib Res* 4: 383–390, 1994.

Ross J, Concetta Morrone M, and Burr DC. Compression of visual space before saccades. *Nature* 386: 598–601, 1997.

Schlag J and Schlag-Rey M. Through the eye, slowly: delays and localization errors in the visual system. *Nat Rev Neurosci* 3: 191–215, 2002.

Schlag J, Schlag-Rey M, and Dassonville P. Interactions between natural and electrically evoked saccades. II. At what time is eye position sampled as a reference for the localization of a target? *Exp Brain Res* 76: 548–558, 1989.

Schlag-Rey M, Schlag J, and Shook B. Interactions between natural and electrically evoked saccades. I. Differences between sites carrying retinal error and motor error signals in monkey superior colliculus. *Exp Brain Res* 76: 537–547, 1989.

Snyder LH, Grieve KL, Brotchie P, and Andersen RA. Separate body- and world-referenced representations of visual space in parietal cortex. *Nature* 394: 887–891, 1998.

Sommer MA and Wurtz RH. A pathway in primate brain for internal monitoring of movements. *Science* 296: 1480–1482, 2002.

Sommer MA and Wurtz RH. What the brain stem tells the frontal cortex. II. Role of the SC-MD-FEF pathway in corollary discharge. *J Neurophysiol* 91: 1403–1423, 2004.

Sparks DL and Mays LE. Spatial localization of saccade targets. I. Compensation for stimulation-induced perturbations in eye position. *J Neurophysiol* 49: 45–63, 1983.

Stahl JS. Eye–head coordination and the variation of eye-movement accuracy with orbital eccentricity. *Exp Brain Res* 136: 200–210, 2001.

Stricanne B, Andersen RA, and Mazzoni P. Eye-centered, head-centered, and intermediate coding of remembered sound locations in area LIP. *J Neurophysiol* 76: 2071–2076, 1996.

Tanaka M. Contribution of signals downstream from adaptation to saccade programming. *J Neurophysiol* 90: 2080–2086, 2003.

Umeno MM and Goldberg ME. Spatial processing in the monkey frontal eye field. I. Predictive visual responses. *J Neurophysiol* 78: 1373–1383, 1997.

Van Gisbergen JAM, Robinson DA, and Gielen S. A quantitative analysis of generation of saccadic eye movements by burst neurons. *J Neurophysiol* 45: 417–442, 1981.

Van Opstal AJ and Hepp K. A novel interpretation for the collicular role in saccade generation. *Biol Cybern* 73: 431–445, 1995.

Vidal PP, Roucoux A, and Berhoz A. Horizontal eye position-related activity in neck muscles of the alert cat. *Exp Brain Res* 46: 448–453, 1982.

Vliegen J, Van Grootel TJ, and Van Opstal AJ. Dynamic sound localization during rapid eye-head gaze shifts. *J Neuroscience* 24: 9291–9302, 2004.

Volle M and Guitton D. Human gaze shifts in which head and eyes are not initially aligned. *Exp Brain Res* 94: 463–470, 1993.

Walker MF, Fitzgibbon EJ, and Goldberg ME. Neurons in the monkey superior colliculus predict the visual result of impending saccadic eye movements. *J Neurophysiol* 73: 1988–2003, 1995.

Xing J and Andersen RA. Models of the posterior parietal cortex which perform multimodal integration and represent space in several coordinate frames. *J Cogn Neurosci* 12: 601–614, 2001.

Zipser D and Andersen RA. A back-propagation programmed network that simulates response properties of a subset of posterior parietal neurons. *Nature* 331: 679–684, 1988.